AD_____

Award Number: DAMD17-01-1-0728

TITLE: Development and Novel Uses of Antibodies in Epithelial
Ovarian Cancer

PRINCIPAL INVESTIGATOR: Daniel Meruelo, Ph.D.

CONTRACTING ORGANIZATION: New York University School of Medicine
New York, NY 10016

REPORT DATE: September 2004

TYPE OF REPORT: Final

PREPARED FOR: U.S. Army Medical Research and Materiel Command
Fort Detrick, Maryland 21702-5012

DISTRIBUTION STATEMENT: Approved for Public Release;
Distribution Unlimited

The views, opinions and/or findings contained in this report are
those of the author(s) and should not be construed as an official
Department of the Army position, policy or decision unless so
designated by other documentation.

20050407 191

REPORT DOCUMENTATION PAGE

Public reporting burden for this collection of information is estimated to average 1 hour per response, including the time for reviewing instructions, searching existing data sources, gathering and maintaining the data needed, and completing and reviewing this collection of information. Send comments regarding this burden estimate or any other aspect of this collection of information, including suggestions for reducing this burden to Washington Headquarters Services, Directorate for Information Operations and Reports, 1215 Jefferson Davis Highway, Suite 1204, Arlington, VA 22202-4302, and to the Office of Management and Budget, Paperwork Reduction Project (0704-0188), Washington, DC 20503

1. AGENCY USE ONLY (Leave blank)	2. REPORT DATE September 2004	3. REPORT TYPE AND DATES COVERED Final (15 Aug 2001 – 14 Aug 2004)

4. TITLE AND SUBTITLE
Development and Novel Uses of Antibodies in Epithelial Ovarian Cancer

5. FUNDING NUMBERS
DAMD17-01-1-0728

6. AUTHOR(S)

Daniel Meruelo, Ph.D.

7. PERFORMING ORGANIZATION NAME(S) AND ADDRESS(ES)
New York University School of Medicine
New York, NY 10016

E-Mail: merued01@med.nyu.edu

8. PERFORMING ORGANIZATION REPORT NUMBER

9. SPONSORING / MONITORING AGENCY NAME(S) AND ADDRESS(ES)

U.S. Army Medical Research and Materiel Command
Fort Detrick, Maryland 21702-5012

10. SPONSORING / MONITORING AGENCY REPORT NUMBER

11. SUPPLEMENTARY NOTES

12a. DISTRIBUTION / AVAILABILITY STATEMENT
Approved for Public Release; Distribution Unlimited

12b. DISTRIBUTION CODE

13. ABSTRACT (Maximum 200 Words)

We studied the therapeutic value of Sindbis vectors for advanced metastatic ovarian cancer by using two mouse models; a SCID xenograft model growing human ES-2 ovarian cancer cells, and a syngeneic C57BL/6 model growing mouse MOSEC ovarian cancer cells. Imaging, histological, and molecular data demonstrated that Sindbis vectors systemically and specifically kill metastasized tumors in the peritoneal cavity, leading to significant suppression of the carcinomatosis in both animal models. Utilization of different bioluminescent markers for imaging studies demonstrated an excellent correlation between vector and tumor localization *in vivo*. Sindbis vector suppression of murine MOSEC tumor cells indicate that Sindbis tumor specificity is not attributable to a species difference between human tumor and mouse normal cells. Sindbis virus infects mammalian cells using the 67-kDa laminin receptor (LAMR). Immunohistochemical staining indicates that LAMR is elevated in tumor vs. normal cells. Down-regulated expression of LAMR with siRNA significantly reduces the infectivity of Sindbis vectors. Thus, tumor overexpression of the LAMR may explain the specificity and efficacy that Sindbis vectors. Incorporation of cytokine genes such as interleukin-12 and interleukin-15 genes enhances the vector's efficacy. Sindbis viral vectors may be promising agents for both specific detection and suppression of metastatic ovarian cancer.

14. SUBJECT TERMS

Sindbis vector, ovarian cancer, in vivo imaging

15. NUMBER OF PAGES
20

16. PRICE CODE

17. SECURITY CLASSIFICATION OF REPORT Unclassified	18. SECURITY CLASSIFICATION OF THIS PAGE Unclassified	19. SECURITY CLASSIFICATION OF ABSTRACT Unclassified	20. LIMITATION OF ABSTRACT Unlimited

Table of Contents

BODY: INTRODUCTION

Despite aggressive surgical approaches and combination chemotherapeutic regimens implemented over the past two decades, epithelial ovarian cancer remains a disease with a grim prognosis. Because early symptoms of ovarian cancer are uncommon and if present, non-specific, the majority of patients are diagnosed with stage III or IV disease which is characterized by carcinomatosis throughout the peritoneal cavity. Current treatment combines surgery, which can be both diagnostic and therapeutic, and systemic chemotherapy. The therapeutic goal of surgical management in ovarian cancer is optimal cytoreduction; however, in the most advanced cases, such cytoreductive surgery may not be technically possible. Furthermore, although 70% of ovarian cancer patients initially respond to platinum-based chemotherapy, the majority experience recurrence, and overall five-year survival is approximately 20% for advanced stage disease (1). New therapeutic approaches are clearly warranted.

Our laboratory has been developing a Sindbis viral vector system for the treatment of cancer. Sindbis virus is a member of the alphavirus genus in the Togaviridae family. In nature, Sindbis virus is transmitted via mosquito bites to mammals. Thus, Sindbis virus has evolved as a blood-borne vector. This hematogenous delivery property of Sindbis virus enables Sindbis vectors to reach tumor cells throughout the circulation (2, 3). Another advantageous property of Sindbis vectors is that they have been shown to induce apoptosis in mammalian cells (4-7). This cytotoxicity could eradicate cancer if specific and complete targeting is achieved.

The cell specificity of Sindbis vectors may be mediated by the 67-Kda high affinity laminin receptor (LAMR) (8, 9), which is over-expressed in several types of human tumors including those of ovarian origin (10-17). We hypothesized that intraperitoneal (i.p.) delivery of Sindbis vectors may be especially suitable for detection and treatment of ovarian cancer because this cancer predominantly involves the peritoneal cavity, and because human ovarian cancer cells also overexpresses LAMR (15). Assisted by the IVIS Imaging System®, specific detection of metastases could be achieved by Sindbis vectors carrying bioluminescent luciferase genes in small animals.

We utilized two highly reproducible and clinically accurate mouse models of ovarian cancer. The first is a SCID xenograft model which uses human ES-2 cells derived from a clear cell ovarian carcinoma that is known for its resistance to a variety of chemotherapeutic agents, including cisplatin. We also used a syngeneic ovarian cancer model developed by Roby *et al.* (18), which entails injecting MOSEC cells into fully syngeneic immunocompetent C57BL/6 mice. In both models, Sindbis vectors specifically targeted tumor cells and effectively suppressed disease progression. Successful tumor targeting in the MOSEC model allowed us to demonstrate that the tumor specificity of Sindbis vectors is not due to preferential tropism for human cells and that immune responses did not affect the targeting or therapeutic efficacy of Sindbis vectors. In addition, by using two different bioluminescent reporter genes to label ES-2 tumor cells

1

and Sindbis vectors, a highly significant correlation has been established, for the first time, between the locations of metastases and vector infection.

MATERIALS AND METHODS

Cell lines: ES-2 cells were obtained from the American Type Culture Collection (ATCC, Manassas, VA) and were cultured in McCoy's 5A medium (Mediatech, Inc., Herndon, VA) supplemented with 10% FBS. ES-2/Fluc cells are derived from the ES-2 line by stable transfection of a plasmid, pIRES2-Fluc/EGFP, as described previously (3). A hairpin siRNA sequence targeting 5'-CCAGAUCCAGGCAGCCUUC-3' of the human laminin receptor precursor (LRP) transcript was designed using the on-line insert design tool (www.ambion.com, Ambion Inc. Austin, TX) and was ligated into the BamHI site on pSilencer™ 2.1-U6 hygro plasmid (Ambion Inc.). The siRNA expression cassette was excised from pSilencer™ 2.1-U6 hygro plasmid using the PvuII restriction enzyme and was sub-cloned into the AflII site on the pIRES2-Fluc/EGFP plasmid. The plasmid, named pIRES2-Fluc/EGFP/αLRP, was then stably transfected into ES-2 cells to generate the ES-2/Fluc/αLRP cell line. The mouse ovarian MOSEC cell line (clone ID8) was a generous gift from Dr. Katherine F. Roby at University of Kansas Medical Center, Kansas City, and was maintained in Dulbecco's modified Eagle's medium (DMEM) supplemented with 4% FBS and 1× ITS (Insulin-Transferrin-Selenium, Mediatech).

Production of Sindbis vectors: Various Sindbis vectors were produced by electroporation of both replicon RNA (SinRep5) and helper RNA (DH-BB) into BHK cells as described previously (3). The Renilla luciferase (Rluc) gene was excised from the phRL-CMV plasmid (Promega Co., Madison, WI) and inserted into the Xba I site of the SinRep5 plasmid (Invitrogen Co., San Diego, CA) for Sindbis/Rluc vector production. A similar procedure was performed to generate the Sindbis/IL-15 vector, which carries a mouse IL-15 gene obtained from the pORF-mIL-15 plasmid (InvivoGen Co.).

β-galactosidase activity assay: We infected 3×10^5 ES-2/Fluc or ES-2/Fluc/αLRP cells on 12-well plates with Sindbis/LacZ vectors at MOI of 100, 10, or 1. After 1 hr incubation at room temperature, cells were washed with PBS and cultured in αMEM/5% FBS. The next day, cells were lysed with 200 μL of M-PER® lysis buffer (Pierce Biotechnology, Rockford, IL). We added 50 μL of the cell lysates into 50 μL of All-in-One Beta-Galactosidase Assay Reagent (Pierce Biotechnology) and incubated at room temperature for 5 min prior to reading at 405 nm. For each designed MOI three independent assays were performed and the data presented as the percentage of activities compared with infected ES-2/Fluc cells.

Animal models: C.B-17-SCID mice (female, 6-8 week old, Taconic, Germantown, NY) were i.p. injected with 2×10^6 ES-2 cells in 0.5 mL McCoy's 5A medium on day -5. On day 0, both ES-2 inoculated mice and tumor-free control mice received a single treatment of Sindbis/Fluc vector and the bioluminescence signals were monitored using the IVIS® system 100 series (Xenogen Corp., Alameda, CA) the next day (day 1) as described

previously (3). Some mice received a second i.p. treatment of Sindbis/Fluc vector on day 2 and were IVIS imaged again on day 3.

For colocalization experiments, SCID mice were i.p. inoculated with 1.5×10^6 ES-2/Fluc cells on day 0 and received one i.p. treatment of Sindbis/Rluc vector ($\sim 10^7$ PFU in 0.5 mL of OptiMEM I) on day 5. The next day (day 6), we determined the Rluc activities in anesthetized mice by i.p. injection of 0.3 mL of 0.2 mg/mL coelenterazine (Biotium, Inc., Hayward, CA) followed by a 5 min IVIS® imaging duration. The bioluminescence generated by Rluc is short-lived and gradually fades away within 30 min (19). After 30 min, the same mice were i.p. injected with 0.3 mL of 15mg/mL D-luciferin (Biotium, Inc) and a second IVIS® imaging for Fluc activity was performed. We used Living Image® software (Xenogen Corp.) to grid the imaging data and integrate the total bioluminescence signals in each boxed region.

We i.p. injected 1×10^7 murine MOSEC cells into C57BL/6 mice (female, 6-8 week old, Taconic, Germantown, NY) to induce advanced ovarian cancer (18). 4 weeks after inoculation, mice were i.p. treated with Sindbis/Fluc and were imaged with IVIS® system the next day. Tumor-free control mice were treated with SinRep/Fluc and imaged in parallel. In order to visualize the specific targeting of Sindbis/Fluc to MOSEC metastases, we i.p. treated the tumor-bearing mice 7 weeks after tumor inoculation and imaged the next day. All animal experiments were performed in accordance with NIH and institutional guidelines.

Tissue sections and slide preparation: Hematoxylin and eosin staining of tissue sections were performed as described previously (3). Immunohistochemistry was performed on formalin fixed paraffin embedded tissues for LAMR detection. Tissue sections (5 μm thick) were prepared onto charged glass slides, baked for 2 hours at 40°C. They were deparaffinized and rehydrated in a phosphate buffered saline solution. Antigen retrieval was performed by boiling in 1 mM EDTA (pH = 8) buffer solution for 10 minutes. Tissue sections were incubated with the polyclonal rabbit primary antibody AB711 (1:100 dilution, Abcam Ltd., Cambridge, UK) at room temperature overnight. Detection was performed using an alkaline phosphatase system (Vectastain® ABC-AP kit, Vector laboratories, Burlingame, CA) with the secondary antibody diluted at 1:250 and sections were incubated at room temperature for 30 minutes. Hematoxylin was used as a counter stain.

Real-time RT-PCR: 1000, 500, or 250 ng of total cellular RNA obtained from ES-2/Fluc or ES-2/Fluc/αLRP cells was reverse-transcribed (RT) into cDNA for 1 hr at 42°C in a 20 μL reaction mixture containing 15 units of ThermoScript™ RNAse H⁻ Reverse Transcriptase (Invitrogen Co.). Real-time quantitative PCR was performed on a iCycler iQ real-time PCR detection system (Bio-Rad, Hercules, CA) in a 20 μl reaction mix containing 4 μL RT product, reaction buffer (1×), dNTPs (200 μM/each), human GAPDH or LAMR primers (0.5 μM/each), 1U of Taq Polymerase (Fisher Scientific, Pittsburgh, PA), fluorescein (100 nM) and 1μl of SYBR Green I (10,000× diluted to

1:75,000 v/v). Thermocycling was carried out over 40 cycles of 30 s at 95°C, 30 s at 60°C and 1 min at 72°C. The sequences of the primers used were as following:

hLAMR forward primer (on exon 2): 5'-CTCAAGAGGACCTGGGAGAAGC-3'
hLAMR reverse primer (on exon 3): 5'-TGGCAGCAGCAAACTTCAGC-3'
hGAPDH forward primer: 5'-CACCAGGGCTGCTTTTAACTCTGGTA-3'
hGAPDH reverse primer: 5'-CCTTGACGGTGCCATGGAATTTGC-3'

hGAPDH was chosen as the housekeeping gene for comparative analysis. The fold change in LAMR relative to the GAPDH endogenous control was determined by: fold change = $2^{-\Delta(\Delta C_T)}$, where $\Delta C_T = C_{T(LAMR)} - C_{T(GAPDH)}$, and $\Delta(\Delta C_T) = \Delta C_{T(ES\text{-}2/Fluc/\alpha LRP)} - \Delta C_{T(ES\text{-}2/Fluc)}$. C_T is the threshold cycle determined at 84°C for fluorescence data collection.

RESULTS

Sindbis vectors specifically target ES-2 metastases throughout the peritoneal cavity.

I.p. injection (on day 0) of Sindbis/Fluc, which carries a Fluc gene, enabled the specific infection/detection of ES-2 metastases in SCID mice. In ES-2 inoculated mice, we observed substantial vector infection in regions corresponding to the pancreas/omentum, bowel and peritoneal fat (Fig. 1A, right panel). Low levels of Sindbis/Fluc infection were observed in the lower abdomen of some tumor-free control mice (Fig. 1A, left panel). We performed another set of IVIS® imaging after the removal of the peritoneum to examine the exact location of vector infection in both control and ES-2 inoculated mice (Fig. 1B, day 1).

To determine if repeated administration of Sindbis vectors leads to accumulative infection in tumor-free mice, we i.p. injected a second dose of Sindbis/Fluc vector to both control and ES-2 inoculated mice on day 2 and performed IVIS imaging on day 3. Interestingly, control mice that receive the second Sindbis/Fluc injection showed no detectable IVIS signal in the peritoneal cavity while the vector infection signal in tumor metastases remained high in the ES-2 inoculated mice (Fig. 1B, day 3). We histologically confirmed the specific vector infection in tumor metastases in several tissues/organs, such as peritoneal fat, peritoneum, diaphragm, pancreas, and the bowel (Fig. 1C, organs harvested from same mouse (ES-2 day 3) in Fig. 1B). In tumor-free control mice, except for the transient background signals observed in the fatty tissue after the first treatment, no vector infection signal was detected in the peritoneal cavity. ES-2 inoculated mice that received only a single Sindbis/Fluc treatment on day 0 showed decreased bioluminescence signals in tumors on day 3 compared with those treated twice (data not shown). Increased bioluminescence signals in twice treated mice suggest that while a single vector treatment is capable of detecting widespread metastases in the peritoneal cavity, it is not sufficient to infect all tumor cells within the same metastatic implant. Successful Sindbis cancer therapy will probably require repetitive treatments in order to achieve good therapeutic effects.

We histologically confirmed the presence of tumor metastases within several tissues of the peritoneal cavity at this early stage of disease progression, including

4

pancreas, omentum, mesentery, and the peritoneum (Fig. 1*D*). Four weeks after tumor inoculation, we also observed lung micrometastases of ES-2 tumors (Fig. 1*D*). The lung metastases may be established via the lymphatic pathway since we observed the presence of tumor in the mediastinal lymph nodes of the chest (data not shown).

To establish the degree and specificity of Sindbis infection of tumor cells we conducted imaging studies that measured independent bioluminescent signals from tumor cells and vectors. Since the ES-2/Fluc cells express the firefly luciferase gene, we generated a Sindbis vector, Sindbis/Rluc, which carries a different luciferase gene cloned from soft coral *Renilla renifomis* (Rluc) for IVIS® imaging. Firefly luciferase uses D-luciferin while *Renilla* luciferase uses coelenterazine to generate bioluminescence; the two luciferases are highly substrate specific and do not cross-react (19). By switching substrates we separately determined the Rluc (Fig. 2, left) and Fluc activities (Fig. 2, right) *in vivo* using the IVIS® system. For quantitative analysis, the bioluminescence signals generated, in the same animal, from Sindbis/Rluc and ES-2/Fluc were quantitated using Living Image® software. The images of Rluc and Fluc signals were grided ($12\times8 = 96$ boxed regions) and corresponding regions were analyzed for statistical correlation. A highly significant correlation was established ($P<0.0001$). Thus, data analysis indicate that a single i.p. delivery of Sindbis vectors leads to efficient infection of the metastasized tumor cells throughout the peritoneal cavity.

It is known that Sindbis virus induces cytopathic effects in infected mammalian cells, which results from its ability to induce apoptosis (4-7). We also observed increased caspase-3 activity within ES-2 cell after Sindbis infection (data not shown). Therefore, we compared the efficacy of Sindbis vectors carrying different gene payloads against metastatic ovarian cancer in ES-2/Fluc models. Three different vectors were tested: Sindbis/LacZ, which carries the bacterial β-galactosidase gene; Sindbis/IL-12, which carries mouse IL-12 genes; and Sindbis/IL-15, which carries a mouse IL-15 gene. IL-12 and IL-15 are known to elicit anti-tumor activity by activation of natural killer (NK) cells (20, 21). On day 0, all SCID mice were i.p. inoculated with 1.5×10^6 ES-2 cells and daily treatments were started on day 1. Control mice did not receive vector treatment. Total whole body photon counts were determined by IVIS® imaging on day 1, 5, 13, and 20 to determine disease progression of ES-2/Fluc metastases (Fig. 3*A*) (3). Without any anti-tumor cytokine gene, the Sindbis/LacZ vector significantly suppressed disease progression compared with untreated control mice (Fig. 3*B*, two-way ANOVA: $P < 0.0001$). The IL-12 and IL-15 cytokine genes further enhanced the anti-tumor activity of Sindbis vectors compared with mice treated with Sindbis/LacZ (Fig. 3*B*, two-way ANOVA: $P = 0.0081$ for Sindbis/IL-12 and $P = 0.0026$ for Sindbis/IL-15). Within 5 days, the Sindbis/IL-12 treatments reduced the tumor load by, on average, more than 11 fold to ~140,000 tumor cells (Fig. 3*B*). This signifies a reduction of greater than 95% when compared to untreated mice, while, the increase in photon counts indicated that the number of cells by day 5 had increased, on average, 1.9 fold to ~3×10^6 tumor cells. These results suggest that, in addition to specific infection/detection, repeated vector treatments suppress tumor growth likely via induction of apoptosis. Furthermore, incorporation of anti-tumor genes into this vector system further enhances the efficacy against tumors.

Sindbis vectors specifically target mouse MOSEC ovarian cancer metastases in a syngeneic animal model.

The advanced ovarian cancer model described above was established by inoculation of human ES-2 cells into SCID mice that rapidly developed advanced disease. In this model, the possibility that the tumor specific infection results from a preferential tropism of Sindbis vectors for human cells could not be rule out. Further, as SCID mice lack intact immune systems, this model does not assess the impact of potential immune responses on delivery and targeting of Sindbis vectors to tumor cells. We took advantage of a previously established syngeneic ovarian cancer model in C57BL/6 immunocompetent mice (18). I.p. inoculation of MOSEC cells into C57BL/6 mice induces a disease similar to that induced by i.p. injection of ES-2 cells into SCID mice, albeit the MOSEC cells grow more slowly in animals. Four weeks after i.p. MOSEC inoculation, the mice received a single i.p. treatment of Sindbis/Fluc. Tumor-free control mice also received Sindbis/Fluc treatment. As had been the case in the ES-2/Fluc SCID model, we observed substantial bioluminescent signals indicating widespread metastasis in the peritoneal cavity of tumor-inoculated mice (Fig. 4A). No significant bioluminescent signals were generally observed, although low background signals in the peritoneal fat were observed, sometimes in control mice. In order to visualize the specific infection in tumor metastases, we used a C57BL/6 mouse bearing MOSEC tumors for 7 weeks. At this later time point, ascites were visible (Fig. 4B, left panel) and extensive tumor metastases were visually observed during autopsy (Fig. 4B, lower right panel). When given a single i.p. injection of Sindbis/Fluc vectors, the whole body imaging revealed a weaker bioluminescent signal than mice treated four weeks after tumor inoculation, which probably results from the development of severe ascites which decreases the excitation and subsequent detection of luminescent signals and that vector dosage must infect a much larger area and is thus less concentrated. Sindbis/Fluc vector demonstrated specific targeting to most of the MOSEC metastases within the peritoneal cavity (Fig. 4B, upper right panel). In addition, the vector could efficiently infect metastases in several tissues, similar to the ES-2 model (Fig. 4C). Tumor metastases were confirmed histologically on these tissues (Fig. 4D).

We found, in addition to specific detection, Sindbis vectors suppress disease progression. Mice treated with Sindbis/Fluc have lower incidence of ascites after two weeks of treatments (7 weeks after tumor inoculation). By then, 5/7 untreated control mice developed severe ascites compared to only 1/8 in Sindbis/Fluc mice (Fig. 5A). In addition, the treated mouse with ascites was considerably less sick. Disease suppression was also reflected in significant prolongation of survival in Sindbis-treated mice (Fig. 5B).

LAMR expression levels correlate with the infectivity of Sindbis vectors.

LAMR has been identified as the cell surface receptor for Sindbis infection to mammalian cells (8, 9). To establish whether our data is consist with the hypothesis that Sindbis vectors preferentially infect tumor vs. normal cells due to differences in LAMR expression, we performed immunohistochemical staining on tumor sections with an antibody specific to the laminin receptor precursor (LRP). The ES-2/Fluc tumors express higher levels of LAMR than normal tissues (Fig. 6A). Similarly, we also observed higher

6

levels of LAMR expression in MOSEC metastases and spontaneous tumors in MSV-RGR/p15$^{+/-}$ transgenic mice (Fig. 6A), which are also targeted by Sindbis vectors (3).

To further investigate the correlation between LAMR expression and Sindbis vector infection, we generated an ES-2 derived cell line, ES-2/Fluc/αLRP, that stably expresses a siRNA specifically against LRP messenger in addition to the plasmid backbone for Fluc expression as in ES-2/Fluc cells. We performed real-time RT-PCR to determine the expression levels of LAMR in ES-2/Fluc and ES-2/Fluc/αLRP cells. A pair of primers specific to human GAPDH mRNA was included to serve as an internal control. Our results indicate that the LAMR expression level in ES-2/Fluc/αLRP cells is about 40% compared with ES-2/Fluc cells (Fig. 6B). To determine the Sindbis infectivity of these two cell lines, we infected ES-2/Fluc and ES-2/Fluc/αLRP cells with Sindbis/LacZ vectors at MOI of 100, 10, and 1. As hypothesized, ES-2/Fluc/αLRP cells that express less LAMR are infected less well by Sindbis vectors compared with ES-2/Fluc (Fig. 6C). These data indicate that the Sindbis infectivity of ES-2 cells correlates with the expression levels of LAMR and are concordant with previously reports that indicated LAMR as the mammalian receptor for Sindbis infection (8, 9).

FIGURE LEGENDS

Fig. 1. Sindbis vector specifically infects metastasized ES-2 cancer cells throughout the peritoneal cavity. *A,* SCID mice were inoculated with 2×10^6 ES-2 cells on day −5 and were i.p. treated with a single injection of Sindbis/Fluc vector on day 0. On the next day (day 1) the bioluminescence signals, resulting from vector infection of ES-2 cancer cells, were monitored using the IVIS® system (right panel). Low level of background vector infection was observed in the lower abdomen of tumor-free control mice (left panel). *B,* After the first whole body IVIS® imaging on day 1, the peritoneum was removed for another IVIS® imaging of the peritoneal cavity. Despite a low level of infection in the peritoneal fat tissue of tumor-free control mouse, specific tumor infection of Sindbis/Fluc vector was observed throughout the peritoneal cavity of ES-2 inoculated mouse upper panels). Some mice received a second i.p. injection of Sindbis/Fluc vector on day 2 and we IVIS® imaged the peritoneal cavities on day 3 (lower panels). The background infection in the fat tissue disappeared completely and no detectable signals were observed elsewhere in the peritoneal cavity of control mouse. In contrast, Sindbis/Fluc vector infection was sustained in the ES-2 tumor metastases. *C,* The organs in the double-treated ES-2 inoculated mouse (lower right panel in 2B) were harvested and imaged. Specific vector infection was exclusively observed in ES-2 metastases. The tumor metastases are shown in red circles. Similar specific tumor targeting was also observed in ES-2 inoculated mice that received only a single Sindbis/Fluc treatment (data not shown). *D,* Corresponding tumor metastases (indicated by arrows) were observed microscopically at this early stage of disease progression in the omentum/pancreas, bowel, and peritoneum. We also observed lung metastases four weeks after ES-2/Fluc inoculation. Bar: 500 μm.

Fig. 2. Sindbis/Rluc infection co-localized with the metastasized ES-2/Fluc tumors in the peritoneal cavity as determined by the IVIS® system. SCID mice were i.p. inoculated with 1.5×10^6 ES-2/Fluc cells. Five days later while the disease was still microscopic,

inoculated mice received a single i.p. treatment of Sindbis/Rluc vectors and were imaged the next day. The first IVIS® imaging was done by i.p. injection of Rluc substrate, coelenterazine, followed by a 5 min acquiring interval (left panel). 30 min after the coelenterazine injection, when the short-lived Rluc signals faded away, Fluc substrate, D-luciferin, was i.p. injected to determine the ES-2/Fluc tumor locations (right panel).

Fig. 3. Sindbis vectors suppress disease progress in mice inoculated with ES-2/Fluc cells. **A**, 1.5×10^6 ES-2/Fluc cells were i.p. inoculated into SCID mice on day 0. Next day (day 1), mice were imaged using the IVIS® Imaging System using D-luciferin as substrate and were split into four groups: control ($n = 12$), that received no vector treatment and Sindbis/LacZ ($n = 9$), Sindbis/IL-12 ($n = 5$) and Sindbis/IL-15 ($n=4$) groups that received daily i.p. treatments of corresponding Sindbis vectors. All Sindbis treatments suppressed the tumor growth on the mesentery and diaphragm, and reduced the signals on the omentum compared with control mice. The signals by the left legs at the lower abdomens were intramuscular tumors at tumor inoculation sites. **B**, Quantitative analysis of the whole body total photon counts of control and Sindbis treated mice. Error bars represent the s.e.m.

Fig. 4. Sindbis/Fluc vectors are capable of specific detection of syngeneic MOSEC metastases in the peritoneal cavity of immunocompetent C57BL/6 mice. **A**, Four weeks after i.p. inoculation with 1×10^7 MOSEC cells, mice were treated with a single i.p. injection of Sindbis/Fluc vectors and were IVIS® imaged the next day. Tumor-free control mice were treated with Sindbis/Fluc and imaged in parallel. Substantial bioluminescent signals were observed in the peritoneal cavities of MOSEC-inoculated mice but not in the ones of control mice. **B**, In order to visualize the specific tumor infection, a single i.p. injection of Sindbis/Fluc vector was administered to C57BL/6 mice bearing MOSEC tumors for 7 weeks. By then the mice showed the onset of ascites development and had severe carcinomatosis that was directly visible during necropsy. The left panel shows the whole body imaging the day after a single i.p. Sindbis/Fluc treatment and the right panels show imaging of the peritoneal cavity of the same animal. The tumor metastases are shown in red circles. **C**, The imaging of the organ array indicated that Sindbis/Fluc vector specifically infects MOSEC metastases on the peritoneum (1), bowel/mesentery (2), small and great omentum (4), next to stomach and spleen, liver surface (5), kidney (6), peritoneal fat (7), diaphragm (8), and uterus (9). No substantial signals were observed in the heart (3), lung (3) and brain (10). Red circles indicate the MOSEC metastases locations visible with regular light photography. **D**, Microscopically, H&E staining confirmed the presence of MOSEC tumors (indicated by arrows) on the pancreas, peritoneal fat, mesentery, and diaphragm. Bar: 250 μm.

Fig. 5. Sindbis vector treatments suppress disease progression of C57BL/6 mice i.p. inoculated with MOSEC cancer cells. Mice were i.p. inoculated with 1×10^7 MOSEC cells on day 0 and the daily i.p. treatments of Sindbis/Fluc vector started on day 34. Control mice received no Sindbis treatment. **A**, On day 47, 5/7 control mice have severe ascites compared to only 1/8 in Sindbis/Fluc mice whose ascites was much less intense. **B**, The survival curves of different treatment group. Sindbis/Fluc significantly prolonged the survival mice carrying MOSEC cancer (Sindbis/Fluc vs. control: $P<0.0071$, log rank test).

8

Fig. 6. Infectivity of Sindbis vectors correlated with the expression of LAMR. *A*, Immunohistochemical staining on tumor sections with an antibody specific to the laminin receptor precursor (LRP) of LAMR revealed that tumor metastases (indicated by arrows) over-express LAMR in both ES-2/Fluc and MOSEC models. Similarly, we also observed high levels of LAMR expression in spontaneous tumors in MSV-RGR/p15$^{+/-}$ transgenic mice, which were successfully targeted by Sindbis vectors as demonstrated previously (3). Bar: 250 μm. *B*, ES-2/Fluc/αLRP cells, that stably expresses a siRNA specifically against LRP messenger, had a lower expression level of LAMR as indicated by real-time RT-PCR assay. A pair of primers specific to human GAPDH mRNA was also included to provide an internal control. The graph represents the average of three independent assays using 1000, 500, 250 ng of total RNA, and the error bar indicates the standard error of the means (s.e.m.). *C*, To determine the Sindbis infectivity of these two cell lines, we infect ES-2/Fluc and ES-2/Fluc/αLRP cells with Sindbis/LacZ vectors at MOI of 100, 10, and 1. The β-galactosidase activities in infected cells were analyzed the day after infection. For each designed MOI three independent assays were performed and the data were present as the percentage of activities in infected ES-2/Fluc cells.
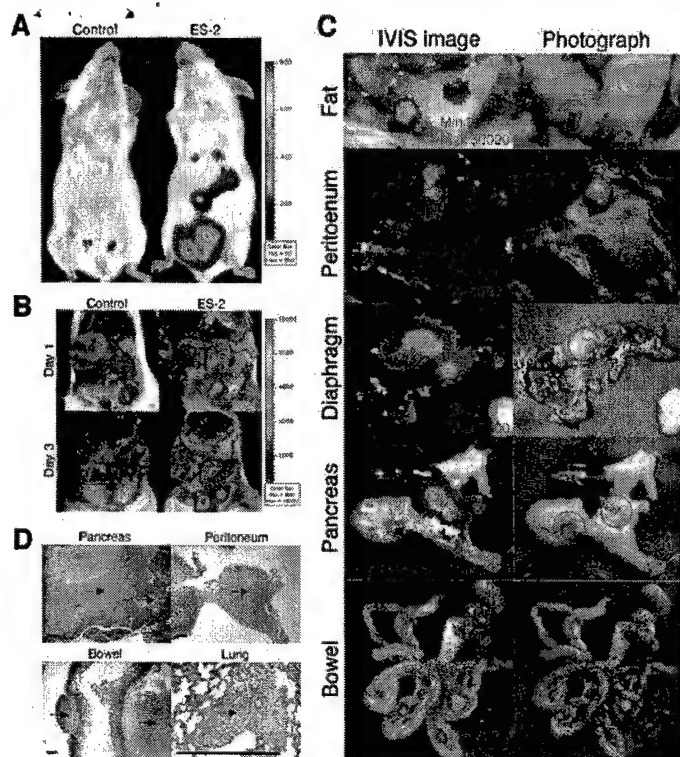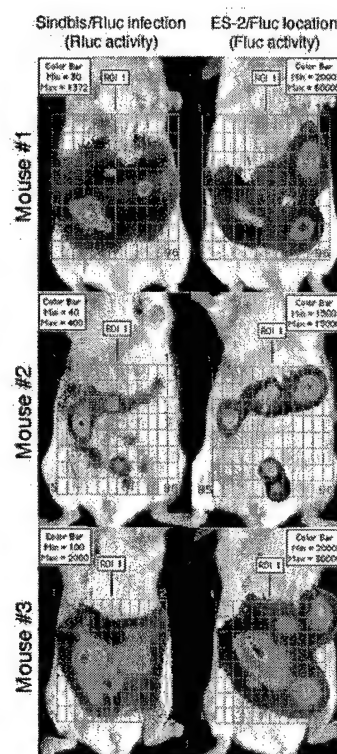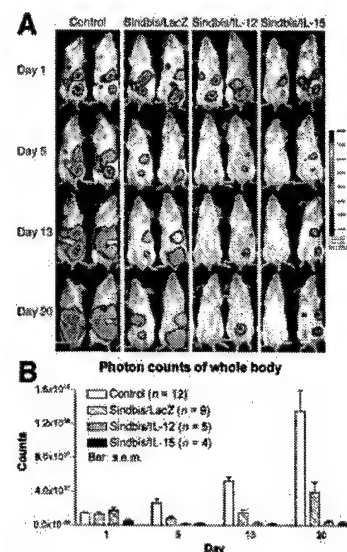
Figure 1

Figure 2

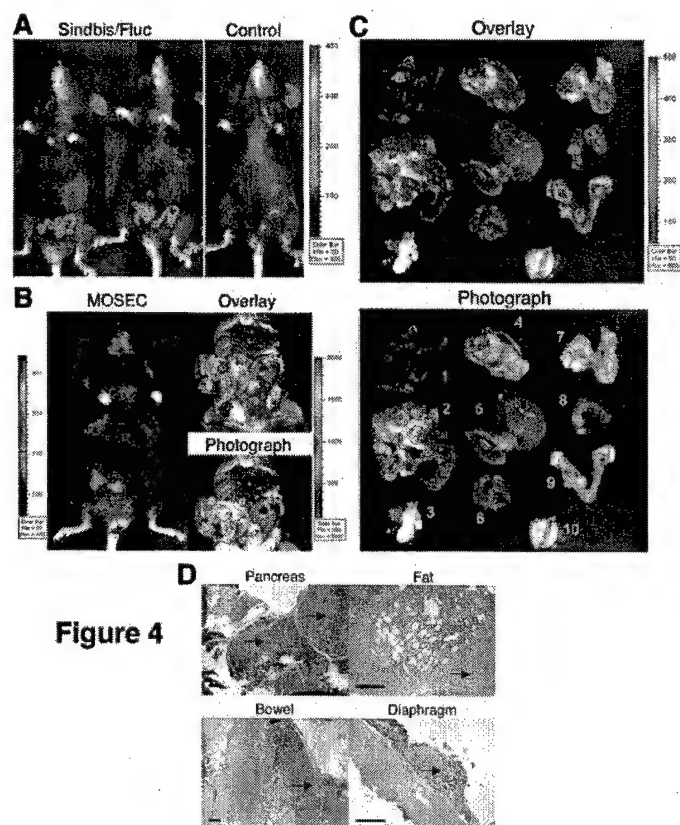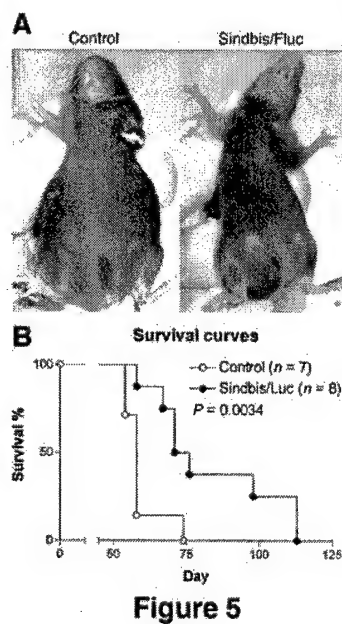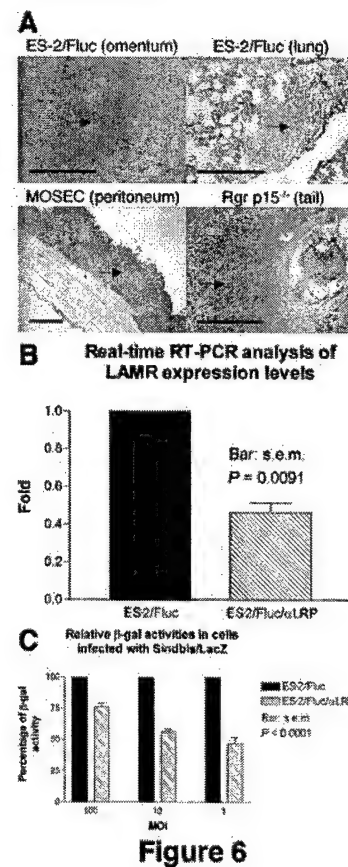**Figure 3**

Figure 4

Figure 5

Figure 6

KEY RESEARCH ACCOMPLISHMENTS:

- Generated of safe, targetable Sindbis vectors that have the potential for direct *in vivo* therapies.

- Demonstrated that it is possible to generate packaging cell lines for the continuous production of Sindbis vectors.

- Demonstrated that Sindbis vectors mediate potent anti-tumor activity *in vivo*.

- Used Sindbis viral vectors for specific detection and suppression of advanced ovarian cancer in animal models.

REPORTABLE OUTCOMES:

1. Meruelo, D., B. Levin, and C. Pampeno. Generation of safe, targetable Sindbis vectors that have the potential for direct *in vivo* therapies. *In* "Vector Targeting for Therapeutic gene Delivery" (David T Curiel and Joanne T. Douglas, Eds.), Wiley & Sons, Inc, New York. Pp 353-375, 2002.

2. Tseng J., B. Levin, T. Hirano, H. Yee, C. Pampeno, and D. Meruelo Sindbis vectors mediate potent anti-tumor activity *in vivo*. JNCI 94:1790-1802, 2002.

3. Ishizu A, Tsuji T, Abe A, Saito S, Takahashi T, Ikeda H, Meruelo D, Yoshiki T Transduction of Dominant Negative ATF-1 Suppresses The pX gene expression in joint fibroblastic cells derived from HTLV-1 transgenic rats. Experimental and Molecular Pathology 74:309-313, 2003.

4. Blank, M., M. Mandel, Y. Keisari, D. Meruelo and G. Lavie. Enhanced Hsp90 ubiquitinylation as a potential mechanism for mitotic cell death in cancer cells. Cancer Research, 63:8241-2847, 2003.

5. Tseng J., B. Levin, A. Hurtado, H. Yee, I. Perez de Castro, M. Jimenez, P. Shamamian, R. Jin, R. P. Novick, A. Pellicer and D. Meruelo. Systemic tumor targeting and killing by Sindbis viral vectors. Nature (Biotechnology) 22:70-77, 2004

6. Lavie. G, L. Trakhtenbrot, M. Mandel, D. Meruelo, M. Blank, Y. Mazur, S. Hazn, and G. Rechavi. Cell cycle arrest associated with dysregulation of selected S-Phase Checkpoints induced by dimethyl tetramethoxy helianthrone. Int. J. Cancer 111:596-603, 2004.

7. Meruelo, D. Systemic gene therapy by Sindbis vectors: A potentially safe and effective targeted therapy for identifying and killing tumor cells in vivo. Discovery Medicine 4:54-57, 2004.

8. Tseng JC, Hurtado A, Yee H, Levin B, Boivin C, Benet M, Blank SV, Pellicer A, Meruelo D. Using Sindbis viral vectors for specific detection and suppression of advanced ovarian cancer in animal models. Cancer Res. 64:6684-6692,2004

CONCLUSIONS: In this report, we demonstrate the capability of Sindbis viral vectors to specifically infect and detect micro and macro tumor metastases in the peritoneal cavity. The advantage of Sindbis viral gene therapy vectors for tumor detection is that the vector can markedly amplify the signals by over-expression of the transgene markers. While luciferase expression may not be suitable for imaging of tumor cells in humans, because of the potential greater depths at which such cells might be found in humans *versus* mice, other more tissue penetrating reporter genes, such as the herpes simplex virus type-1 thymidine kinase (HSV1-tk) and dopamine-2 receptor (D_2R) genes, can be incorporated into Sindbis vectors for tumor detection using positron emission topography (PET) (22).

In order to specifically detect tumor cells, viral vector systems require either tumor specific receptors for infection or, alternatively, the use of tumor specific promoters for reporter transgene expression in tumor cells. In general, vectors using tumor-specific promoters for gene activation are taken up and expressed by only a small proportion of the targeted tumor cells. In contrast, because vectors based on Sindbis virus infect via a ubiquitously expressed receptor that is differentially expressed between tumor and normal cells, these vectors achieve efficient tumor targeting and robust transgene expression using the viral promoter. Sindbis vectors rapidly and extensively amplify transgenes once they infect target cells. Sindbis vectors thus provide faster and more sensitive detection of tumor cells via systemic administration. In addition, our imaging data, along with previous biochemical analysis of transgenes expression (2), indicates that no Sindbis vector infection of liver or other organs occurs in mice upon systemic delivery, permitting the use of relatively high doses of Sindbis vectors capable of suppressing metastatic tumor growth.

The cell surface receptor for Sindbis has been identified as the high affinity LAMR (8), a glycosylated membrane protein that mediates cellular interactions with the extracellular matrix, and it is over-expressed and unoccupied (compared to normal cells) in the vast majority of tumors (23-26). Several reports suggest that higher levels of LAMR on human tumor cells provide growth advantages such as more aggressive invasiveness and metastatic spread (10-14). This fortuitous event also provides a differential marker on the surface of normal and tumor cells for Sindbis attachment and infection.

LAMR is an attractive target on ovarian cancer cells since they have been shown to express high levels of this receptor (15-17). In our advanced ovarian cancer models, both ES-2/Fluc and MOSEC cells express higher levels of LAMR than normal tissues (Fig. 6A) and can be specifically infected by Sindbis vectors (Fig. 1 and 4). Similar higher expression levels of LAMR were also observed in spontaneous tumors of MSV-

RGR/p15$^{+/-}$ transgenic mice, which were also targeted by Sindbis vectors (3). In the peritoneal cavity, it is likely that most of the LAMRs on the tumor cells in the ascetic fluid are not occupied by the ligand laminin, and therefore serve as ideal targets for Sindbis vector infection. The observation that Sindbis treatments suppressed ascites formation in this study supports this point of view.

Although the exact composition of LAMR is still unknown, one essential component of the LAMR has been identified as a 37-kDa laminin receptor precursor (LRP) (27). It is believed that LRP is modified post-translationally and forms heterodimers (28) with other glycosylated proteins prior to translocation to the cell surface. One of its likely partners is heparan-sulfated proteoglycan (HSPG) (29). It is relevant to note that a number of laboratories have also identified the LAMR as the target for prion protein (29-34). For example, Hundt *et al.* (29) have shown that the prion protein binds to two sites of this LAMR. One of the binding sites is dependent for optimal binding in the presence of a heparan sulfate arm of a HSPG molecule, but the other binding site appears to function independently of heparan sulfate.

It has been proposed that heparan sulfate plays a role in the attachment of Sindbis vectors to cells (35). However, while the interaction with heparan sulfate enhances the infection efficiency, it is not required for infection (35). Therefore, it is possible that the Sindbis vectors infect tumor cells via interactions with both LRP and heparan sulfate. The exact nature of the receptor is an issue that requires further study if a comprehensive understanding of the anti-tumor activities of Sindbis vectors is to be achieved.

Our data indicate that the tumor specificity of Sindbis vectors is not likely to be due to a different tropism between human and mouse cells. The vector is as capable of specific infection/detection of murine MOSEC ovarian cancer cells (Fig. 4) as it is of human ES-2/Fluc cells in SCID mice (Fig. 1). In addition, Sindbis vectors can specifically infect spontaneous tumors in MSV-RGR/p15$^{+/-}$ transgenic mice (3). Since no human cells are involved in the latter model, the specific infection of Sindbis vector is likely due to fundamental differences between normal and tumor cells such as expression levels of LAMR.

Infection of Sindbis vector induces apoptosis without any cytotoxic transgene *in vitro* (4-7) and *in vivo* (2). Despite the cytotoxicity to infected cells, systemic delivery of Sindbis vectors shows no observable morbidity in our experimental animals.

In most cases, after wild type replication-capable Sindbis virus enters the bloodstream, virus titers reach high levels throughout all organs (36, 37). Yet, minimal, self-limiting disease (usually no more than one week in duration and accompanied only by mild symptomology) is associated with the wild-type virus (36, 37). While maintaining the capability of reaching all organs through the bloodstream, it has been shown that the laboratory strain of Sindbis used to produce all of our vectors does not cause any disease or adverse consequences in humans (36, 37). One reason for this is that all our vectors are replication defective. That is, once these vectors infect cells they cannot propagate to other cells. While they are able to infect virtually all target cells, the fact that they do not replicate and do not integrate makes them very safe.

14

In tumor-free mice, we only observed very low levels of vector infection in the peritoneal fat after the initial i.p. vector treatment. For reasons that require further investigation, this low level infection resolved after a subsequent vector treatment. That is, no infection is detectable in normal mice after the second injection of Sindbis vectors. In contrast, specific tumor infection persists during the course of treatments. Since these phenomena occur in SCID mice, which are immunodeficient, the loss of vector infection in normal fat tissues may be due to other innate anti-viral responses, such as type I interferon (IFN-I) production, which protect surrounding normal tissues from secondary vector infection. Several studies suggest that, during oncogenesis, tumor cells evolve to be less responsive to interferon stimuli compared with normal cells (38). Therefore, it is plausible that after the initial vector infection IFN-I production is induced, protecting the normal fat tissue from secondary infection. On the other hand, tumors, which often demonstrate defects in IFN-I response, are still subject to secondary Sindbis vector infection and eventually succumb to the vector cytotoxicity. In this aspect, the difference in the responsiveness of IFN-I may provide Sindbis vectors another level of specificity for tumor cells.

All our present studies were done with replication-defective vectors. It is plausible to argue that use of a replication-capable vector system could enhance the anti-tumor effects. However, we believe that this will not be necessary with Sindbis vectors. Rather, we hope that additional studies or combination of Sindbis vectors with other agents will allow us to develop protocols that can achieve complete eradication of ovarian tumor cells. Sindbis vectors have a decisive safety advantage over replication competent viruses for use in gene therapy. Hopefully, these vectors can be developed without having to sacrifice this advantage.

In conclusion, we have shown, in our aggressive mouse ovarian cancer models, that Sindbis vectors can achieve two major therapeutic goals of cancer gene therapy: specific detection of tumor cells, primary and metastatic, and efficient tumor suppression. Additional studies with a variety of gene payloads are underway. For all the reasons stated, Sindbis vectors appear to offer much promise for the treatment of advanced ovarian cancer.

REFERENCES:

1. Fishman DA, Bozorgi K. The scientific basis of early detection of epithelial ovarian cancer: The national ovarian cancer early detection program (NOCEDP). In: Stack MS, Fishman DA, editors. Ovarian cancer. Norwell: Kluwer Academic Publishers; 2002. p.3-28.
2. Tseng JC, Levin B, Hirano T, Yee H, Pampeno C, Meruelo D. In vivo antitumor activity of Sindbis viral vectors. J Natl Cancer Inst. 2002; 94(23): 1790-802.
3. Tseng JC, Levin B, Hurtado A, et al. Systemic tumor targeting and killing by Sindbis viral vectors. Nat Biotechnol. 2004; 22(1): 70-7.

4. Levine B, Huang Q, Isaacs JT, Reed JC, Griffin DE, Hardwick JM. Conversion of lytic to persistent alphavirus infection by the bcl-2 cellular oncogene. Nature. 1993; 361(6414): 739-42.

5. Jan JT, Chatterjee S, Griffin DE. Sindbis virus entry into cells triggers apoptosis by activating sphingomyelinase, leading to the release of ceramide. J Virol. 2000; 74(14): 6425-32.

6. Jan JT, Griffin DE. Induction of apoptosis by Sindbis virus occurs at cell entry and does not require virus replication. J Virol. 1999; 73(12): 10296-302.

7. Balachandran S, Roberts PC, Kipperman T, et al. Alpha/beta interferons potentiate virus-induced apoptosis through activation of the FADD/Caspase-8 death signaling pathway. J Virol. 2000; 74(3): 1513-23.

8. Wang KS, Kuhn RJ, Strauss EG, Ou S, Strauss JH. High-affinity laminin receptor is a receptor for Sindbis virus in mammalian cells. J Virol. 1992; 66(8): 4992-5001.

9. Strauss JH, Wang KS, Schmaljohn AL, Kuhn RJ, Strauss EG. Host-cell receptors for Sindbis virus. Arch Virol Suppl. 1994; 9: 473-84.

10. Martignone S, Menard S, Bufalino R, et al. Prognostic significance of the 67-kilodalton laminin receptor expression in human breast carcinomas. J Natl Cancer Inst. 1993; 85(5): 398-402.

11. Sanjuan X, Fernandez PL, Miguel R, et al. Overexpression of the 67-kD laminin receptor correlates with tumor progression in human colorectal carcinoma. J Pathol. 1996; 179(4): 376-80.

12. de Manzoni G, Verlato G, Tomezzoli A, et al. Study on Ki-67 immunoreactivity as a prognostic indicator in patients with advanced gastric cancer. Jpn J Clin Oncol. 1998; 28(9): 534-7.

13. Taraboletti G, Belotti D, Giavazzi R, Sobel ME, Castronovo V. Enhancement of metastatic potential of murine and human melanoma cells by laminin receptor peptide G: attachment of cancer cells to subendothelial matrix as a pathway for hematogenous metastasis. J Natl Cancer Inst. 1993; 85(3): 235-40.

14. Ozaki I, Yamamoto K, Mizuta T, et al. Differential expression of laminin receptors in human hepatocellular carcinoma. Gut. 1998; 43(6): 837-42.

15. van den Brule FA, Castronovo V, Menard S, et al. Expression of the 67 kD laminin receptor in human ovarian carcinomas as defined by a monoclonal antibody, MLuC5. Eur J Cancer. 1996; 32A(9): 1598-602.

16. van den Brule FA, Berchuck A, Bast RC, et al. Differential expression of the 67-kD laminin receptor and 31-kD human laminin-binding protein in human ovarian carcinomas. Eur J Cancer. 1994; 30A(8): 1096-9.

17. Liebman JM, Burbelo PD, Yamada Y, Fridman R, Kleinman HK. Altered expression of basement-membrane components and collagenases in ascitic xenografts of OVCAR-3 ovarian cancer cells. Int J Cancer. 1993; 55(1): 102-9.

18. Roby KF, Taylor CC, Sweetwood JP, et al. Development of a syngeneic mouse model for events related to ovarian cancer. Carcinogenesis. 2000; 21(4): 585-91.

19. Bhaumik S, Gambhir SS. Optical imaging of Renilla luciferase reporter gene expression in living mice. Proc Natl Acad Sci U S A. 2002; 99(1): 377-82.

20. Perussia B, Chan SH, D'Andrea A, et al. Natural killer (NK) cell stimulatory factor or IL-12 has differential effects on the proliferation of TCR-alpha beta+, TCR-gamma delta+ T lymphocytes, and NK cells. J Immunol. 1992; 149(11): 3495-502.

21. Evans R, Fuller JA, Christianson G, Krupke DM, Troutt AB. IL-15 mediates anti-tumor effects after cyclophosphamide injection of tumor-bearing mice and enhances adoptive immunotherapy: the potential role of NK cell subpopulations. Cell Immunol. 1997; 179(1): 66-73.

22. Yaghoubi SS, Wu L, Liang Q, et al. Direct correlation between positron emission tomographic images of two reporter genes delivered by two distinct adenoviral vectors. Gene Ther. 2001; 8(14): 1072-80.

23. Liotta LA, Horan Hand P, Rao CN, Bryant G, Barsky SH, Schlom J. Monoclonal antibodies to the human laminin receptor recognize structurally distinct sites. Exp Cell Res. 1985; 156(1): 117-26.

24. Barsky SH, Rao CN, Hyams D, Liotta LA. Characterization of a laminin receptor from human breast carcinoma tissue. Breast Cancer Res Treat. 1984; 4(3): 181-8.

25. Terranova VP, Rao CN, Kalebic T, Margulies IM, Liotta LA. Laminin receptor on human breast carcinoma cells. Proc Natl Acad Sci U S A. 1983; 80(2): 444-8.

26. Liotta LA, Rao NC, Barsky SH, Bryant G. The laminin receptor and basement membrane dissolution: role in tumor metastasis. Ciba Found Symp. 1984; 108: 146-62.

27. Rao CN, Castronovo V, Schmitt MC, et al. Evidence for a precursor of the high-affinity metastasis-associated murine laminin receptor. Biochemistry. 1989; 28(18): 7476-86., 1989.

28. Buto S, Tagliabue E, Ardini E, et al. Formation of the 67-kDa laminin receptor by acylation of the precursor. J Cell Biochem. 1998; 69(3): 244-51.

29. Hundt C, Peyrin JM, Haik S, et al. Identification of interaction domains of the prion protein with its 37-kDa/67-kDa laminin receptor. EMBO J. 2001; 20(21): 5876-86.

30. Leucht C, Simoneau S, Rey C, et al. The 37 kDa/67 kDa laminin receptor is required for PrP(Sc) propagation in scrapie-infected neuronal cells. EMBO Rep. 2003; 4(3): 290-5.

31. Gauczynski S, Peyrin JM, Haik S, et al. The 37-kDa/67-kDa laminin receptor acts as the cell-surface receptor for the cellular prion protein. Embo J. 2001; 20(21): 5863-75.

32. Shmakov AN, Bode J, Kilshaw PJ, Ghosh S. Diverse patterns of expression of the 67-kD laminin receptor in human small intestinal mucosa: potential binding sites for prion proteins? J Pathol. 2000; 191(3): 318-22.

33. Rieger R, Edenhofer F, Lasmezas CI, Weiss S. The human 37-kDa laminin receptor precursor interacts with the prion protein in eukaryotic cells. Nat Med. 1997; 3(12): 1383-8.

34. Rieger R, Lasmezas CI, Weiss S. Role of the 37 kDa laminin receptor precursor in the life cycle of prions. Transfus Clin Biol. 1999; 6(1): 7-16.

35. Byrnes AP, Griffin DE. Binding of Sindbis virus to cell surface heparan sulfate. J Virol. 1998; 72(9): 7349-56.

36. Taylor RM, Hurlbut HS. Isolation of coxsackie-like viruses from mosquitoes. J Egypt Med Assoc. 1953; 36: 489-94.

37. Taylor RM, Hurlbut HS, Work TH, Kingsbury JR, Frothingham TE. Sindbis virus: A newly recognized arthropod-transmitted virus. Am J Trop Med Hyg. 1955; 4: 844-46.

38. Stojdl DF, Lichty BD, tenOever BR, et al. VSV strains with defects in their ability to shutdown innate immunity are potent systemic anti-cancer agents. Cancer Cell. 2003; 4(4): 263-75.